Solid-State Electronics 184 (2021) 108110

Contents lists available at ScienceDirect

Solid State Electronics

journal homepage: www.elsevier.com/locate/sse

A phenomenological approach to study the magnetoelectric (ME) response of lead free magnetostrictive $NiFe_2O_4$–Piezoelectric $BaZr_{0.2}Ti_{0.8}O_3$ particulate composites

Pradeep Chavan

Department of Studies in Physics, SB Arts & KCP Science College, Vijayapura 586103, Karnataka, India

ARTICLE INFO

Handling editor: Y. Kuk

Keywords:
Synthesis
Lattice constant
Semiconducting nature
Small polaron model
Magnetic moment and ME voltage coefficient

ABSTRACT

Lead-free magnetoelectric (ME) composites comprises $NiFe_2O_4$ (NFO) and $BaZr_{0.2}Ti_{0.8}O_3$ (BZT) were synthesized by using conventional double sintering solid-state reaction technique and it's structural, electric, dielectric, magnetic and ME properties were studied. The spectra of X-ray diffraction displayed the formation of parent phase and presence of two phases within the composites (ferrite-ferroelectric). DC resistivity as a function of temperature has been studied, it indicates the semiconducting behavior. Frequency dependent dielectric spectra of the composites indicates small polaron hopping model of conduction mechanism. Magnetic measurements at room temperature shows the composites are soft magnetic and such materials reveals M-H hysteresis type behavior. The composite with x = 0.3 showed the highest value of ME voltage coefficient ~3.82 mV/cmOe. Such ME composite materials furnish fabulous chances as prospective lead-free systems for multifunctional device applications.

1. Introduction

ME materials are the composites that exhibit multiferroic properties and they have potential of mutual modification of the magnetization and electric polarization via applied magnetic and electric field, correspondingly [3]. Owing to its technological applications in novel multifunctional devices, the ME phenomena attracts the concentration of materials scientists and researchers worldwide. The simultaneous existence of both ferromagnetic and ferroelectric properties with ME voltage coefficient makes multiferroic materials appropriate for the applications in several devices like AC/DC magnetic flux sensors, ME-RAM, energy harvesters, four state logic memory devices, ME resonators, read heads, transducers, actuators, capacitors, electromagnetic interference filters, multistate memories, storage devices, microwave devices, integrated and multilayer chip inductors, etc [4]. Compared to single-phase ME materials, the composite materials exhibit a better ME voltage coefficient at room temperature owing to the product property. Thus, to realize high values of ME voltage coefficient, proper selection of a ferroelectric material with a high dielectric constant, low dielectric loss, and enormous piezoelectric coefficient and a ferrite material with a high magnetostriction coefficient, saturation magnetization, remnant magnetization, magnetic moment, and coercive field is important [5].

Numerous researchers around the world are studied and reported on lead free particulate composites synthesized via different sintering techniques with different compositions such as NMFO + BZT [1], (x) $Ni_{0.8}Mg_{0.2}Fe_2O_4$-(1-x)$BaZr_{0.8}Ti_{0.2}O_3$ [2], $CoFe_2O_4$–$BaTiO_3$ [13], $NiFe_2O_4$–$BaTiO_3$ [15], $NiZnFe_2O_4$–$BaTiO_3$ [16], $Ba_{0.9}Sr_{0.1}TiO_3$–$Ni_{0.9}Zn_{0.1}Fe_{1.98}O_4$ [18], $Co_{0.7}Mg_{0.3}Fe_{2-x}Mn_xO_4$–$Sr_{0.5}Ba_{0.5}Nb_2O_6$ [19], $(Ba_{0.85}Ca_{0.15})(Zr_{0.1}Ti_{0.9})O_3$–$CoFe_2O_4$ [20], (x)$BaTiO_3$–(1 − x)$Co_{0.7}Fe_{2.3}O_4$ [21], x $(Na_{0.5}K_{0.5})_{0.94}Li_{0.06}NbO_3$ - (1-x)$CoFe_2O_4$ [22], etc. From previous reports, we noticed that the ME voltage coefficient was found at room temperature within the range from 10 to 3300 mV/cmOe [3–7]. Only few research works are administered towards the development of lead-based ME composites which show the most important ME voltage coefficient values within the range from 0.040 to 4.7 V/cmOe [10]. Arti et al. has reported the ME voltage coefficient values of 122 mV/cmOe for particulate PZT-CFO composites [12]. It is observed that the majority of the composites used lead-based ferroelectric (i.e. $PbZrTiO_3$, PZT) constituents in their compositions [8–11]. The majority of particulate ME composites in previous reports are prepared by straight forward direct physical mixing of magnetostrictive and piezoelectric powders obtained separately. Due to the presence of lead element in these composites, they're highly toxic and thus unfavorable for the sensible device applications and also facing growing global restrictions [14].

E-mail address: cpajju@gmail.com.

https://doi.org/10.1016/j.sse.2021.108110
Received 18 November 2020; Received in revised form 31 March 2021; Accepted 31 May 2021
Available online 3 June 2021

In the present report, we synthesized lead-free ferrite-ferroelectric composites via solid-state reaction method. Thus, nickel ferrite preferred as a magnetostrictive segment, they're extremely high magnetostrictive and resistive materials, but the ferroelectric phase $BaZr_{0.2}Ti_{0.8}O_3$ have elevated dielectric permittivity. ME composites may acquire excellent electrical, magnetic, and ME properties. Therefore in the this paper, study of DC resistivity, dielectric constant, AC conductivity, conduction mechanism, magnetic properties and ME voltage coefficient of the composites was reported.

2. Experimental details

The metal oxides NiO, Fe_2O_3, $BaCO_3$, ZrO_2, and TiO_2 (Himedia manufacture) of analytical reagent grade were used for the synthesis. In initiative, the ferrite phase $NiFe_2O_4$ (NFO) and ferroelectric phase $BaZr_{0.2}Ti_{0.8}O_3$ (BZT) were individually synthesized by using conventional double sintering solid-state reaction technique followed by calcination at 800 °C for 8 hrs [1]. In second step, (x) NFO+ (1-x) BZT (x varies from × = 0.1, 0.2 and 0.3) ME composite series were synthesized [1,2]. The powder of ferrite and ferroelectric phases were mixed thoroughly in desired stoichiometric proportions and pressed into the cylindrical pellet type of 10 mm diameter at a pressure of 5 tons/inch^2. The pellets were finally sintered at 1150 °C for 12 hrs in an ambient atmosphere.

3. Characterization details

X-ray diffraction analysis of the synthesized composite samples were carried out via Angle Dispersive X-ray Diffractometer (ADXRD) (Model: Image plate MAR345, RRCAT Indore) using synchrotron radiation with the energy 15 keV and wavelength 0.80034 Å (Bragg angle: $10° \leq 2\theta \leq 60°$). SEM images of the composite samples were recorded using JEOL-JSM-6390LV to investigate the surface morphology, microstructure and grain size distribution. Using two probe technique, DC resistivity with respect to temperature was measured using KEITHLEY electrometer (Model: 2000).To study the dielectric properties, an LCR meter bridge (Model: PSM1700) at room temperature within the frequency range from 20 Hz to 1 MHz is employed. The magnetic parameters of the composite samples were determined with the help of M-H hysteresis loop which was recorded using vibrating sample magnetometer (VSM) (Model: 735, Lakeshore, National Physical Laboratory, New Delhi). To study the ME output of the composites at room temperature, KEITHLEY electrometer (Model: 2000, National Physical Laboratory, New Delhi) was used to measure the electric field produced across the composite samples by applying a DC magnetic field of about 8.0 kOe.

4. Results and discussion

Fig. 1 represents the XRD spectra of synthesized (x) $NiFe_2O_4$ + (1-x) $BaZr_{0.2}Ti_{0.8}O_3$ (x = 0.1, 0.2 & 0.3) composites. X-ray diffraction pattern of all the composites was assembled into two sets of well-defined peaks, one belongs to the cubic spinel structure of ferrite phase (i.e. 311 peak) and another belongs to the tetragonal perovskite structure of the ferroelectric phase (i.e. 011 peak) [1,2,9,41]. No intermediate phase or additional peaks were identified within the spectra indicating that no significant chemical reaction occurred at the ferrite-ferroelectric interface during the final sintering of the composite samples [17]. Meanwhile, the dependence of diffraction peak intensity on a fraction of ferrite-ferroelectric phase was observed.

X-ray diffraction pattern confirmed the polycrystalline structure with the mixture of cubic spinel-tetragonal perovskite structure; whereas the cubic spinel structure has the space group of Fd-3 m and tetragonal perovskite structure has the space group P4mm [23]. The lattice constants of the ferrites and ferroelectrics were estimated and listed in table 1.

Despite the very fact that the estimated average lattice constant of ferrite phase of 8.35 Å was observed and the average lattice constants of ferroelectric phase a = 4.037 and c = 4.037 were observed. The difference between the tetragonal ratio (c/a = 1 (constant)) shows that there have been no structural variations observed during the preparation and final sintering of the ferroelectric phase. Thus, porosity is the intrinsic possessions in ceramic materials that are synthesized by sintering and powder processing. The high rate of sintering to the composite samples with large crystallite size reduces the porosity and density significantly [24]. The porosity of the composites was estimated by using the Adams and Hendricks method through the relation as follows [40],

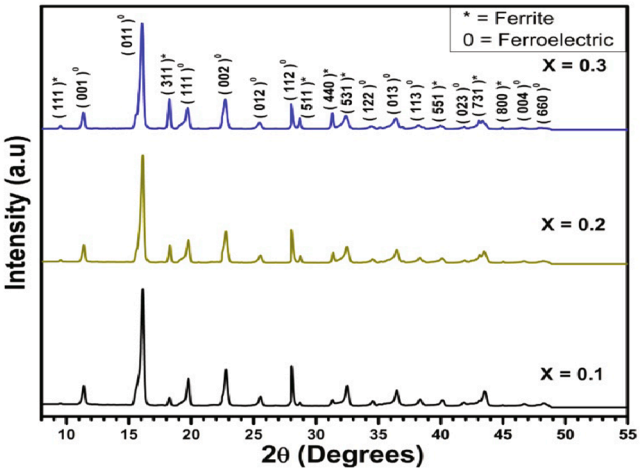

Fig. 1. XRD graph of (x) NFO+ (1-x) BZT ME composites.

Table 1
Lattice parameters, porosity and average grain size of (x) NFO+ (1-x) BZT ME composites.

x content	Lattice Parameters				% Porosity	Average Grain Size (μm)
	Ferrite Phase (Å)	Ferroelectric Phase (Å)				
	a	a	c	c/a		
0.1	8.34	4.037	4.037	1.000	12.41	2.29
0.2	8.35	4.037	4.037	1.000	11.48	2.36
0.3	8.36	4.048	4.047	1.000	10.66	2.48

$$\%\text{Porosity} = \frac{(d_x - d_a)}{d_x} \times 100 \quad (1)$$

Where d_x = X-ray density, d_a = Actual density.

From table 1, the decrease of porosity with increasing mole% of ferrite in composites was observed; it is because of the occurrence of pores that cracks the magnetic circuit between the grains of the composites. The utmost porosity 12.41% was observed for (0.1) NFO + (0.9) BZT composites. Hence, the pores material provides an insulating path to the electrons leading to the rise of resistivity with porosity which intern affects the ME response of the composites. Average grain size of the samples was estimated by Cottrell's method [18] as it gives the relationship between number of intercepts of grain boundary per unit length (P_L) and total number of intercepts (n) i.e.

$$P_L = \left(\frac{n}{2\pi r}\right) \times M \quad (2)$$

Where n: number of grains inside the circle
r: radius of the circle
M: Magnification factor at which SEM micrograph is scanned

The average grain diameter of ferrites was estimated by using the relation:

$$L = \frac{1}{P_L - 1} \quad (3)$$

Fig. 2 shows the SEM micrographs of ME composites (x) NFO + (1-x) BZT sintered at 1150 °C. Well distinct and crystallized dark and light phase regions are often easily identified and that corresponds to the ferrite and ferroelectric phases respectively. Ferrite grains are embedded homogeneously among the ferroelectric matrix [25]. The micrographs suggest that the samples are well sintered, dense and every sample exhibits well defined randomly oriented grains with minimum porosity. The shape and distribution of grains confirmed the polycrystalline nature of the sintered samples. The typical grain size of the composites was estimated by using Cottrell's method [18] and the values of grain sizes were listed in table 1.

It is observed that the average grain size increases with increasing ferrite content in composites. Thus, the substitution of the ferrite phase promotes increasing the grain size with little porosity. From SEM micrographs, it is clear that more number of ferrite grains appears in composites with increasing ferrite content. Thus, the rise in ferrite grain to grain contact shunts the resistance of ferroelectric grains thereby decreasing the effective resistance of the composites. In ME composites, the average grain size increases with decreasing grain surface area; it is because of the grain surface area behaves like an obstacle for the motion of domain walls [19]. The increase of average grain size with increasing ferrite content in composites revealed that the increase of mean free path of the electrons and therefore causes the growth in dielectric constant. However, the tiny amount of grain size of the ferroelectrics compared to ferrites can effectively decrease the outflow of electrical charges induced by the chain formation of ferrite grains in composites [26]. It is significant to spotlight that the well-defined interface between magnetostrictive and piezoelectric phase is crucial to yield a robust ME response in composites.

Fig. 3 shows the variation of DC resistivity with respect to temperature for various compositions of the composites. It is observed that DC resistivity decreases with increasing temperature and it reveals the performance of semiconducting behavior. It is because of the thermally activated drift mobility of electrical charge carriers consistent with the hopping mechanism of conduction electrons. In Fig. 3, DC resistivity graph shows two sections, the primary section is observed at a lower

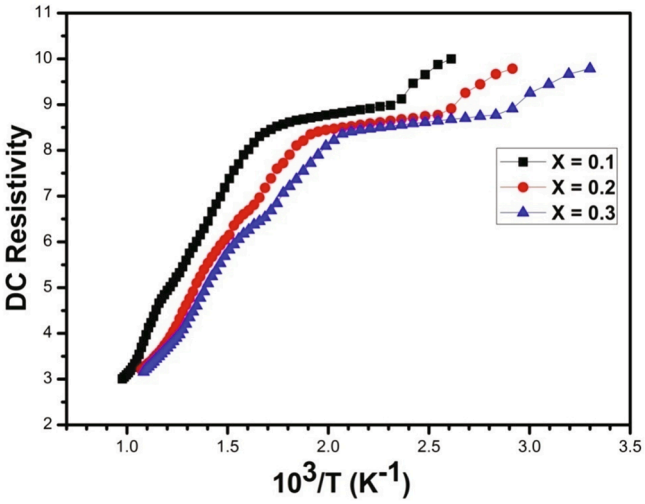

Fig. 3. Variation of DC electrical resistivity with respect to temperature of (x) NFO+ (1-x) BZT composites.

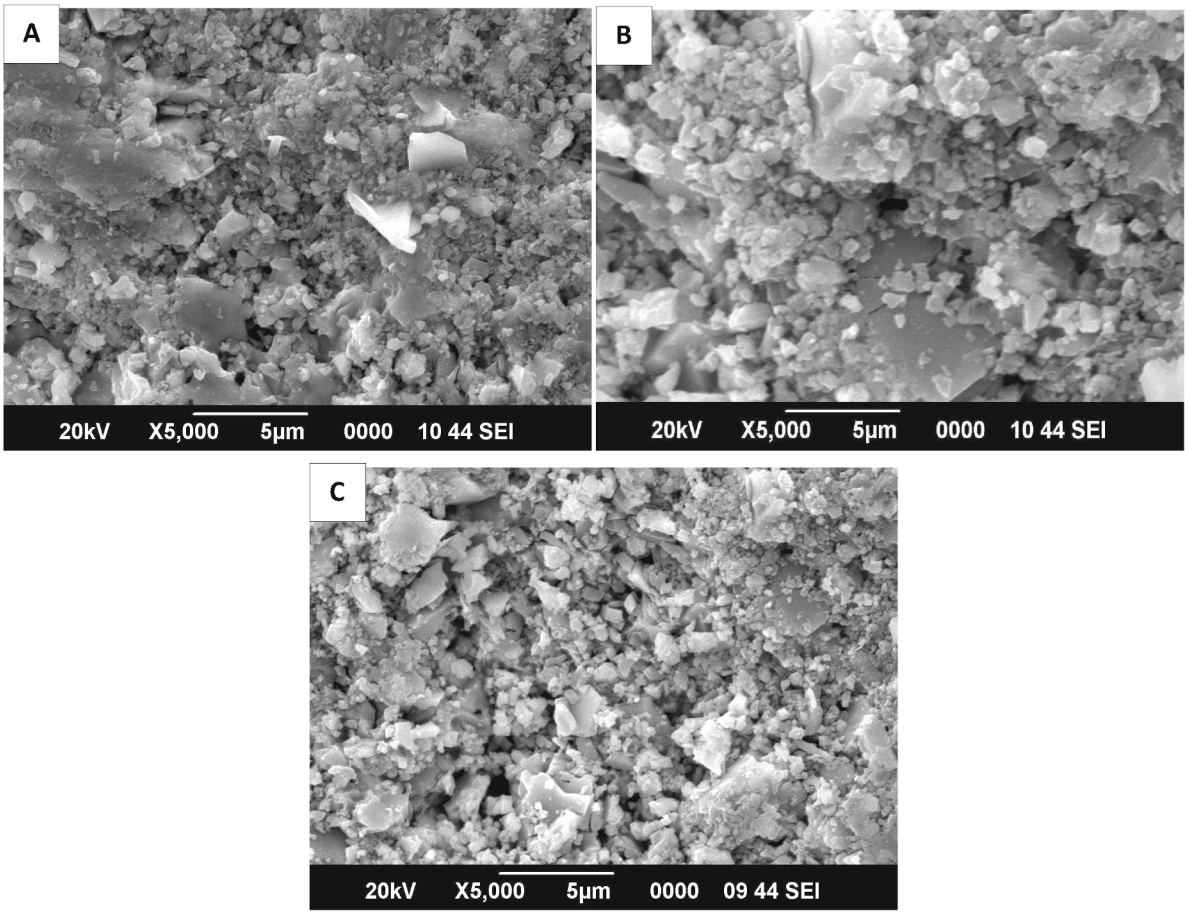

Fig. 2. SEM micrographs of (x) NFO+ (1-x) BZT composites (A = 0.1, B = 0.2 and C = 0.3).

Table 2
Transition temperature and activation energies of paramagnetic and ferromagnetic regions of ME composites.

x content	Activation Energy (eV) Above T_c (Paramagnetic)	Below T_c (Ferromagnetic)	Transition Temperature
	(x) NFO+ (1-x) BZT		
0.1	1.6234	0.1446	235
0.2	1.2708	0.1204	265
0.3	1.4971	0.0999	275

temperature region (below 300 °C) due to the prearranged state of the ferroelectric phase and the second section is observed at a higher temperature region (above 300 °C) due to the chaotic state of paraelectric phase [1,2,27]. However, the polaron hopping type of conduction mechanism of electrons is valid in ferrites and composites at elevated temperatures (above 300 °C). In composites, DC resistivity is large for (10%) $NiFe_2O_4$ + (90%) $BaZr_{0.2}Ti_{0.8}O_3$ with small grain size, whereas the DC resistivity is small for (30%) $NiFe_2O_4$ + (70%) $BaZr_{0.2}Ti_{0.8}O_3$ with large grain size. Hence, the variation of DC electrical resistivity as a function of temperature was due to the less resistivity of ferrite grains compared to the ferroelectric grains in composites [28]. At low temperature (below 300 °C), the replacement of holes among $Ni^{3+} \leftrightarrow Ni^{2+}$ + e- and $Ba^{3+} \leftrightarrow Ba^{2+}$ + e- are responsible for p-type charge carriers. But at high temperature (above 300 °C), the replacement of electrons among the $Fe^{2+} \leftrightarrow Fe^{3+}$ + e- and $Ti^{3+} \leftrightarrow Ti^{4+}$ + e- are responsible for n-type charge carriers and these two types of charge carriers are the incharge of conduction of electrons in composites [24,25].

The number of ions decreases from Fe^{2+} to Fe^{3+} ions at a prominent temperature in composites. The projected values of the activation energy of all the composites are listed in table 2. The projected value of activation energy (E_1) of paramagnetic region varies from 0.5807 eV to 1.6234 eV and the activation energy (E_2) of ferromagnetic region varies from 0.0362 eV to 0.2603 eV. According to Verwey and de Boer mechanism [26], the conduction mechanism of electrons supported the hopping of electrical charge carriers among the ions of equivalent components present in additional one valence state and arbitrarily dispersed crystallographically over the corresponding lattice sites. Thus, the activation energy of the paramagnetic region is bigger than that of the ferromagnetic region and this is often within the fine conformity with the hypothesis of Irkin and Turor [27]. However, the decrease of activation energy in the ferromagnetic region was due to the spin disordering effect. Hence, the activation energy of all the composites is high

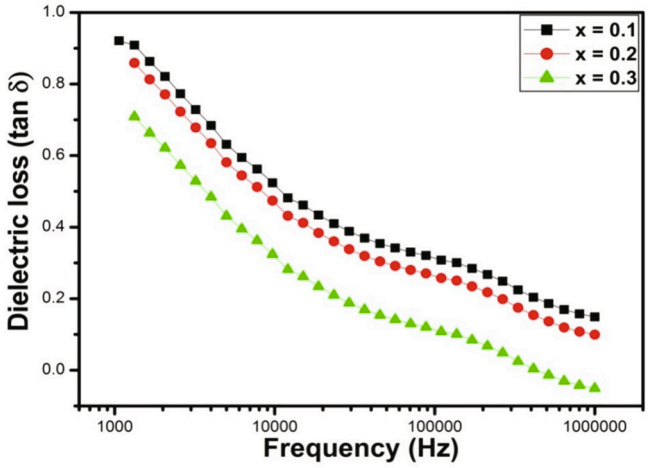

Fig. 5. The variation of dielectric loss tangent graphs of (x) NFO+ (1-x) BZT ME composites.

(>0.2 eV) that shows the polaron hopping type of conduction mechanism. The transition temperature of ME composites was estimated from DC electrical resistivity as a function of temperature graph and is listed in table 2. It is noted that the decrease of transition temperature with increasing mole% of ferrite content in composites was due to the variation in width and chemical composition present in the composites.

The variation of dielectric constant with respect to applied frequency of the composites is shown in Fig. 4. It is observed that the dielectric constant decreases quickly with increasing frequency and then reaches a continuing value at maximum frequency shows the dielectric dispersion behavior. The maximum value of the dielectric constant at minimum frequency region and minimum value of the dielectric constant at maximum frequency region indicates large dielectric dispersion which was due to the Maxwell–Wagner type of interfacial polarization and this is in good agreement with Koop's phenomenological theory [28,29]. The maximum value of dielectric constant was observed at lower frequencies which are explained on the idea of space charge polarization i. e. due to the inhomogeneous dielectric structure; the inhomogeneities within the composites are voids, dislocations, impurities, porosity and grain structure, etc [29]. On the other hand, the elevated value of dielectric constant attributed to the very fact that regions of ferroelectric just in the case of composites are encircled by non-ferroelectric regions like that in the case of relaxor ferroelectric materials; this provides the

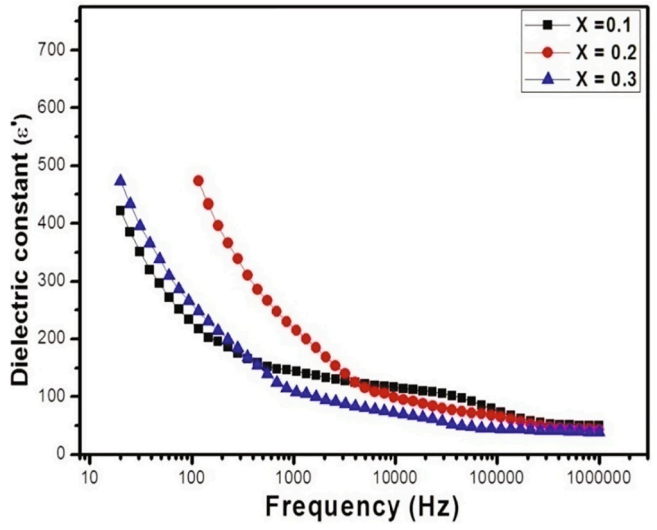

Fig. 4. Variation of dielectric constant with the function of the frequency of (x) NFO+(1-x) BZT composites.

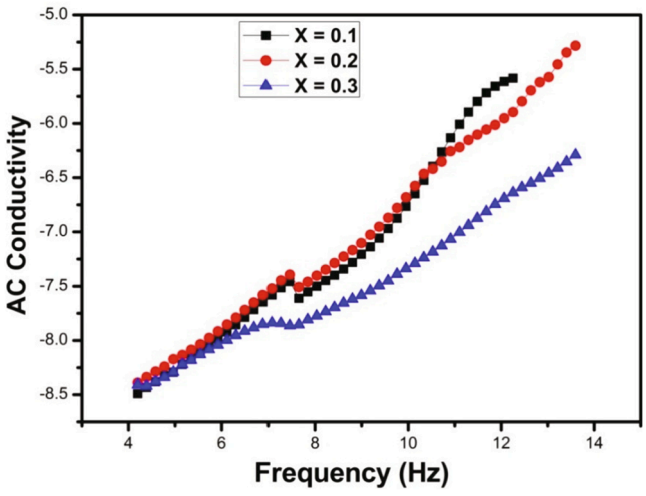

Fig. 6. The variation of AC conductivity with respect to frequency of (x) NFO+ (1-x) BZT composites.

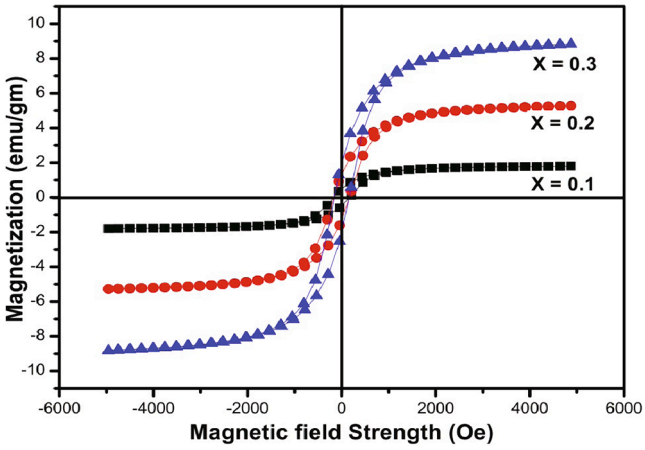

Fig. 7. M-H hysteresis loop of (x) NFO+ (1-x) BZT composites.

rise of the interfacial polarization. The low frequency dispersion behavior contributed to electronic polarization resulting in the polaron hopping type of conduction mechanism [30].

Fig. 5 shows the variation of dielectric loss tangent with frequency at room temperature that is analogous dispersion as that of dielectric constant with respect to frequency.

The hopping of electrons between $Fe^{2+} \leftrightarrow Fe^{3+}$ ions also as $Ni^{2+} \leftrightarrow Ni^{3+}$ ions within the present ferrite system is responsible for the conduction of electrons and this electron hopping causes the local displacements within the direction of the external electric field, influencing dielectric polarization in ferrites [26]. The electron hopping is thermally activated, a rise within the temperature consequences in the increased dielectric polarization, successively causing a rise in the dielectric constant.

Fig. 6 shows the variation of AC conductivity with respect to frequency at room temperature. The variation of AC conductivity is a crucial parameter for understanding the conduction mechanism in materials and it is often explained in terms of polaron hopping type of conduction mechanism among the localized electrons. In a large polaron model, AC conductivity decreases with increasing frequency, while in case of small polaron model the AC conductivity increases with increasing frequency [42]. From Fig. 6, it is observed that AC conductivity increases linearly with increasing frequency that indicates the phenomena of conduction mechanism i.e. due to the small polaron hopping type of conduction mechanism [31].

Hence, the composites obey the small polaron model. A small plateau region is observed in the AC conductivity graph which was attributed to the mixed polarons (small/large) in the conduction of electrons. Therefore, the hopping mechanism is favored in ionic crystal lattices during which a similar type of cation is found in two different oxidation states. The hopping of 3d electrons between Fe^{2+} and Fe^{3+} also Ni^{2+} and Ni^{3+} might play a big role within the conduction mechanism process [32].

Fig. 7 represents the M-H hysteresis loop of (x) NFO + (1-x) BZT (x = 0.1, 0.2 and 0.3) composites. Well saturated magnetic hysteresis loop indicates the ferromagnetic behavior. From Fig. 7, it is observed that each composite sample reveals M-H hysteresis loop behavior at room temperature when a magnetic field of 6 kOe is applied. This behavior of the hysteresis loop confirmed the ordered magnetic nature of the composites i.e. due to the presence of ferrite phase [33]. The magnetic parameters like saturation magnetization (Ms), magnetic moment, coercivity (Hc), and retentivity or remnant magnetization (Mr) for these composite samples were measured from the M-H hysteresis loop and are listed in table 3. It is observed that the saturation magnetization (Ms), magnetic moment, coercive field (Hc) and remnant magnetization increases with increasing ferrite content in composites; it is because of the individual ferrite grains acts like the center of magnetization and saturation magnetization is that the resultant of these individual contributions to the composites.

Also, it is observed that the values of magnetic parameters of composites are small compared to the corresponding values of NFO; it was due to the existence of the non-magnetic ferroelectric phase (B.ZT). However, the magnetic contact increases with ferrite content then the net magnetization increases [34]. Therefore, the highest saturation magnetization 8.6839 emu/gm was achieved for (30%) NFO + (70%) BZT composites. The grains of non-magnetic ferroelectric phase BZT acts like pores in causing the decrease of magnetic strength into the composite samples in presence of applied magnetic field [35].

The coexistence of excellent ferromagnetic and ferroelectric properties within the composites may cause a substantial ME effect. Thus, the ME effect is developed due to the strain-induced in the ferrite phase by an applied magnetic field that is coupled mechanically to induce stress in the bordered ferroelectric phase. The developed result of stress in the polarization of the ferroelectric phase was due to piezoelectricity. ME voltage coefficient was achieved by the electromechanical conversion in the ferroelectric phase and magnetomechanical conversion in the ferrite phase by the transfer of stress through the interface between two phases of the composites [36]. It is well known that strain developed in the ferrite phase increased with the DC magnetic field and saturates in a certain field i.e. because of the magnetostriction. Fig. 8 shows the variation of ME voltage coefficient with respect to the applied magnetic field of the composites and the values are listed in table 3.

It is observed that ME voltage coefficient (dE/dH) decreases with increasing applied magnetic field; it is explained in terms of decrease of DC resistivity with increasing ferrite concentration in composites [37]. From table 3, we noticed that the ME voltage coefficient increases with increasing ferrite content in composites; it is because of the strain produced in NFO and BZT lattices. The highest ME voltage coefficient of 3.82 $mVcm^{-1}Oe$ was observed for (30%) NFO + (70%) BZT composites. The decrease of DC resistivity results in the leakage of charges integrates the ferroelectric phase through ferrite grains. In composites, the ME effect mainly depends on the piezoelectricity of the ferroelectric phase and magnetostriction of the ferrite phase [38]. However, ME composites synthesized with a bit of ferroelectric or ferrite phase consequences the reduction within the effect of piezoelectricity or magnetostriction, correspondingly resulting in the decrease of static ME voltage coefficient with applied DC magnetic field.

In multiferroics, the ME voltage coefficient not only strongly depends on the inherent properties of a private phase but also intimately believes the interfacial elastic coupling between the two phases of the composites. The lowest ME voltage coefficient was observed for × = 0.1 composites because of the comparatively less interface contact and slighter stress transfer area between ferrite and ferroelectric phases in composites. Little contact interface consequences within the least transfer of the induced compressive stress from the ferrite phase to the ferroelectric phase [39]. The induced leakage current makes the dipole alignment harder and deteriorates the ferroelectric and piezoelectric responses, leading to a lower ME voltage coefficient. The massive ME voltage coefficient was attributed to the homogeneous dispersion, enhanced interfacial contact between the two individual phases and modification of the ferroelectric phase with high piezoelectric coefficient [40].

Table 3
Magnetic parameters of (x) NFO+ (1-x) BZT composites.

x content	Saturation magnetization (M_s)	Magnetic moment	Coercivity	Retentivity (M_r)	M_r / M_s	ME output
0.1	1.7876	0.0898	0.0046	0.4945	0.260	1.82
0.2	5.1964	0.2564	0.0058	1.2813	0.247	2.79
0.3	8.8639	0.4205	0.0074	1.8983	0.219	3.82

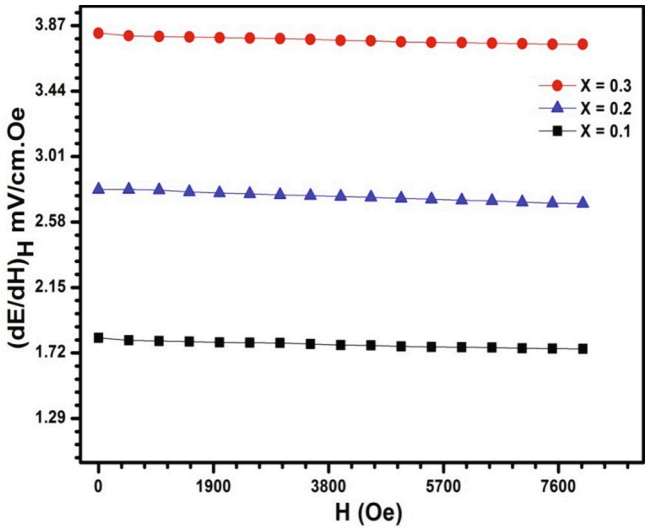

Fig. 8. The variation of ME voltage coefficient with respect to the magnetic field in (x) NFO+ (1-x) BZT composites.

5. Conclusion

ME composite samples were synthesized by the traditional double sintering solid-state reaction technique for the study of various physical properties of the composites. XRD pattern confirmed the formation of a cubic spinel structure of the ferrite phase and tetragonal perovskite structure of the ferroelectric phase. The decrease of DC resistivity with respect to temperature explained the conduction mechanism of electrons supported the hopping of electrical charge carriers. The dielectric constant decreases with increasing applied frequency shows dielectric dispersion behavior. The variation of AC conductivity with frequency is linear which suggested that the conduction was due to the small polaron hopping type of conduction of electrons. The very best saturation magnetization 8.6839 emu/gm was achieved for (30%) NFO + (70%) BZT composites. The highest ME voltage coefficient of 3.82 mV/cmOe was observed for (30%) NFO + (70%) BZT composites. Hence, these composites have better sensitivity within the low-field range.

Declaration of Competing Interest

The authors declare that they have no known competing financial interests or personal relationships that could have appeared to influence the work reported in this paper.

Acknowledgement

Author (Pradeep Chavan) extends his gratitude to Dr. A K Sinha and his team from RRCAT, Indore for their support and cooperation during the experimental measurement of ADXRD at Beamline-12, Indus-II. Author (Pradeep Chavan) grateful to Dr. R K Kotnala and Dr. Jyothi Shah from CSIR National Physical Laboratory, New Delhi for their constant support during the measurement of hysteresis loop using a vibrating sample magnetometer.

References

[1] Pradeep Chavan LR, Naik RKK. Study of electric, magnetic properties and improvements in ME effects of NMFO + BZT particulate composites. J. Magn. Magn. Mater. 2017;433:24.
[2] Pradeep Chavan LR, Naik PBB, Geeta Chavan VT, Muttannavar BK, Bammannavar RKK. Temperature Dependent Electric Properties and Magnetoelectric Effects in Ferroelectric rich Ni0.8Mg0.2Fe2O4 + BaZr0.2Ti0.8O3 Magnetoelectric Composites. J. Alloy. Compds. 2019;777:1258.
[3] Nan CW, Bichurin MI, Dong S, Viehland D, Srinivasan G. Multiferroic magnetoelectric composites: historical perspectives, status and future directions. J. Appl. Phys. 2008;103.
[4] Etier M, Shvartsman VV, Salamon S, Gao Y, Wende H, Lupascu DC. The direct and the converse magnetoelectric effect in multiferroic cobalt ferrite-barium titanate ceramic composites. J. Am. Chem. Soc. 2016;99:3623.
[5] Wang J, Song L, Zhu K, Qiu J. Influence of Zr/Ti atomic ratio and seed layer on the magnetoelectric coupling of Pb(ZrxTi1-x)O3 film on CoFe2O4 bulk ceramic composites. Ceram. International. 2016;42:14431.
[6] Huang S, Deng L, Zhou K, Hu Z, Sun S, Ma Y, Xiao P. Effect of Ag substitution on the electromagnetic property and microwave absorption of LaMnO3. J. Magn. Magn. Mater. 2012;324:3149.
[7] Priya S, Islam R, Dong S, Viehland D. Recent advancements in magnetoelectric particulate and laminate composites. J. Electroceram. 2007;19:149.
[8] Pradhan DK, Chaudary RNP, Nath TK. Magnetoelectric Properties of PbZr0.53Ti0.47O3-Ni0.65Zn0.35Fe2O4 multiferroic composites. Appl. Nanosci. 2012;2:261.
[9] Jiang Q, Liu F, Yan H, Ning H, Libor Z, Zhang KQ, Cain KM, Reece MJ. Magneto-electric properties of multiferroic Pb(Zr0.52Ti0.48)O3-NiFe2O4 nanoceramic composites. J. Am. Ceram. Soc. 2011;94:2311.
[10] Curecheriu LP, Buscaglia MT, Buscaglia V, Mitoseriu L, Postolache P, Ianculescu A, Nanni P. Functional properties of BaTiO3-Ni0.5Zn0.5Fe2O4 magnetoelectric ceramics prepared from powders with core-shell structure. J. Appl. Phys. 2010;107.
[11] Sarkar B, Dalal B, Vishal DA, Kaushik C, Amitava M, De SK. Magnetic properties of BaTiO3-NiFe2O4 composites. J. Appl. Phys. 2014;115.
[12] Zeng M, Wan JG, Wang Y, Yu H, Liu JM, Jiang XP, Nan CW. Resonance magnetoelectric effects in bulk composites of lead zirconate titanate and nickel ferrite. J. Appl. Phys. 2004;95:8069.
[13] Gupta A, Huang A, Shannigrahi S, Chatterjee R. Improved magnetoelectric coupling in Mn and Zn doped CoFe2O4-PbZr0.52Ti0.48O3. Appl Phys. Lett. 2011;98.
[14] [14] Sheng Liu, Lianwen Deng, Shuoqing Yan, HengLuo, Lingling Yao, Longhui He, Yuhan Li, Mingzhong Wu and Shengxiang Huang, Magnetoelectric properties of (80Bi0.5Na0.5TiO3-20Ba0.5K0.5TiO3) Ni0.8Zn0.2Fe2O4 particulate composites prepared by in situ sol-gel. J. Appl. Phys 122 (2017) 034103.
[15] Lisnevskaya IV, et al. Y3Fe5O12/Na, Bi, Sr-doped PZT particulate magnetoelectric composites. J. Magn. Magn, Mater. 2016;405:62.
[16] Bammannavar BK, Naik LR, Pujar RB, Chougule BK. Resistivity dependent magnetoelectric characterization of Ni0.2Co0.8Fe2O4 +Ba0.8Pb0.2Zr0.8Ti0.2O3 composites. J. All. Compds. 2009;477(1):L4.
[17] Kambale RC, Shaikh PA, Rajpure KY, Joshi PB, Kolekar YD. Studies on structural and dielectric properties of CMFO ferrite and BZT ferroelectric magnetoelectric composites. Integ. Ferroelectric. 2010;121(1):1.
[18] Pradeep Chavan, Naik LR, Belavi PB, Chavan GN, Kotnala RK. Synthesis of Bi3+ substituted Ni-Cu ferrites and study of structural, electrical and magnetic properties. J. All. Compds. 2017;694:607.
[19] Lokare SA, Devan RS, Chougule BK. Structural analysis and electrical properties of ME composites. J. Alloys. Compds. 2008;454(1):471.
[20] Babu SN, Srinivas K, Suryanarayana SV, Bhimasankaram T. Magnetoelectric properties in NCMF/PZT particulate and bulk laminate composites. J. Phys D: Appl. Phys. 2008;41(16).
[21] Belavi PB, Chavan GN, Naik LR, Somashekar R, Kotnala RK. Structural, electrical and magnetic properties of cadmium substituted nickel–copper ferrites. J. Mater. Chem. Phys. 2012;132(1):138.
[22] Kadam SL, Patankar KK, Kanamadi CM, Chougule BK. Electrical conduction and magnetoelectric effect in Ni0.50Co0.50Fe2O4+Ba0.8Pb0.2TiO3. Mater. Res. Bull. 2004;39(14):2265.
[23] Pradeep Chavan LR, Naik PBB, Geeta Chavan CK, Ramesha RKK. Studies on Electrical and Magnetic Properties of Mg-Substituted Nickel Ferrites. J. Elect. Mater. 2017;46(1):198.
[24] Kadam SL, et al. Electrical properties and magnetoelectric effect in Ni0.75Co0.25Fe2O4+Ba0.8Pb0.2TiO3 composites. Mater. Chem. Phys. 2003;78:684.
[25] Patil DR, Chougule BK. Effect of resistivity on magnetoelectric effect in (x) NiFe2O4-(1–x)Ba0.9Sr0.1TiO3 ME composites. J. Alloys. Compds. 2009;470:531.

[26] Ryu J, Priya S, Uchino K, Kim H. Magnetoelectric effect in composites of magnetostrictive and piezoelectric materials. J. Electroceramic. 2002;8:107.
[27] Ponpandian N, Balaya P, Narayanasamy A. Electrical conductivity and dielectric behaviour of nanocrystalline NiFe2O4 spinel. J. Phys. Condens. Matter 2002;14:3221.
[28] Bammannavar BK, Naik LR, Pujar RB, Chougule BK. Structural, electrical and magnetic properties of cadmium substituted nickel–copper ferrites. Ind. J. Eng. Mater. Sci. 2007;14:381.
[29] Bammannavar BK, Naik LR. Electrical properties and magnetoelectric effect in (x) Ni0.5Zn0.5Fe2O4 + (1–x) BPZT composites. Smart Mater. Struct. 2009;18.
[30] Kanamadi CM, Das BK, Kim CW, Kang DI, Cha HG, Ji ES, Jadhav AP, Jun BE, Jeong JH, Choi BC, Chougule BK, Kang YS. Dielectric and magnetic properties of (x) CoFe2O4 + (1–x) Ba0.5Sr0.2TiO3magnetoelectric composites. Mater. Chem. Phys. 2009;116:6.
[31] Pradeep Chavan, Naik LR. Effect of Bi3+ ions on the humidity sensitive properties of copper ferrite nanoparticles. Sensors. Actuator. B. Chem. 2018;272:28.
[32] Austin IG, Mott NF. Polarons in crystalline and non-crystalline materials. Adv. Phys. 1969;18:41.
[33] Zhang L, Zhai J, Mo W, Yao X. Dielectric and magnetic properties ofCoFe2O4 − BaTiO3 composite films prepared by a combined method of sol-gel and electrophoretic deposition. J. Am. Ceram. Soc 2010;93(10):3267.
[34] Bhame SD, Joy PA. Effect of sintering conditions and microstructure on the magnetostrictive properties of cobalt ferrites. J Am Ceram Soc 2008;1980:1976.
[35] Wan JG, Liu J-M, Chand HLW, Choy CL, Wang GH, Nan CW. Giant magnetoelectric effect of a hybrid of magnetostrictive and piezoelectric composites. J. Appl. Phys. 2003;93(12):9916.
[36] Chavan P. Chemisorption and Physisorption of Water Vapors on the Surface of Lithium-Substituted Cobalt Ferrite Nanoparticles. ACS Omega 2021;6:1953.
[37] Praveen John Paul, Reddy Monaji Vinitha, Kolte Jayant, Kumar Sakthivel Dinesh, Subramanian Venkatachalam, Das Dibakar. Synthesis, characterization and magnetoelectric properties of (1–x)BCZT-(x)CFO ceramic particulate composites. Int. J. Appl. Ceram. Technol. 2017;14:200.
[38] Li M, Wang Z, Wang Y, Li J. Viehl and D. Giant magnetoelectric effect in self biased laminates under zero magnetic field. Appl. Phys. Lett. 2013;102.
[39] Grossinger R, Duong GV, Sato-Turtelli R. The physics of magnetoelectric composites. J. Magn. Magn. Mater. 2008;320:1972.
[40] Chavan P, Naik LR. Investigation of energy band gap and conduction mechanism of magnesium substituted nickel ferrite nanoparticles. Phys. Stat. Solid. A. 2017;1700077:1.
[41] Devan RS, et al. / Electrical conduction and magnetoelectric effect of (x) BaTiO3 + (1_x)Ni0.92Co0.03Cu0.05Fe2O4 composites in ferroelectric rich region. J. Phys. Chem. Solid. 2006;67:1524.
[42] Fawzi AS, et al. Composition dependent electrical, dielectric, magnetic and magnetoelectric properties of (x)Co0.5Zn0.5Fe2O4 + (1–x)PLZT composites. J. Alloy. Compd. 2010;493:601.

Dr **Pradeep Chavan** obtained M.Sc and Ph.D in physics from Karnatak University, Dharwad, Karnataka, India. He is presently working as Assistant Professor in the Department of Studies in Physics, SB Arts & KCP Science College, Vijayapura-586103, Karnataka, India. His areas of research includes magnetic semiconducting nanomaterials, nanoferrites, ferroelectrics, magnetoelectric composites and humidity sensors.